Behavioural Brain Research 257 (2013) 166–177

Contents lists available at ScienceDirect

Behavioural Brain Research

journal homepage: www.elsevier.com/locate/bbr

Research report

# Quantitative gait analysis of long-term locomotion deficits in classical unilateral striatal intracerebral hemorrhage rat model

Yao Liu[a,b], Li Juan Ao[a], Gang Lu[b,c,*], Elizabeth Leong[b], Qiang Liu[b], Xiao Hong Wang[b,c], Xian Lun Zhu[b], Tin Fung David Sun[b], Zhou Fei[e], Tian Jiu[b], Xiang Hu[b,d], Wai Sang Poon[b,**]

[a] Rehabilitation Department, The Second Affiliated Hospital of Kunming Medical University, Kunming, Yunnan, China
[b] Division of Neurosurgery, Department of Surgery, Prince of Wales Hospital, The Chinese University of Hong Kong, Hong Kong
[c] School of Biomedical Sciences, The Chinese University of Hong Kong, Hong Kong
[d] Shenzhen Beike Cell Engineering Research Institute, Shenzhen, China
[e] Institute of Neurosurgery, Xijing Hospital, Fourth Military Medical University, Xi'an, Shaanxi, China

## HIGHLIGHTS

- We are the first to perform gait analysis on unilateral intracerebral hemorrhage (ICH) rat models.
- We examine long-term gait disturbance in unilateral ICH rats.
- The parameters of print area, stance time, paw pressure, stride length, base of support, and support on style all exhibit change in hemiplegic rats.
- Asymmetry in print area, stance time, and pressure in the contralateral paws of ICH rats lasts for more than one month.
- Brain tissue loss after ICH is significantly related to gait patterns asymmetry.

## ARTICLE INFO

*Article history:*
Received 17 May 2013
Received in revised form
30 September 2013
Accepted 3 October 2013
Available online 12 October 2013

*Keywords:*
Intracerebral hemorrhage
Unilateral striatal impairment
Long term investigation
Gait analysis
Hematoma volume

## ABSTRACT

Gait analysis is a systematic collection of quantitative information on bodily movements during locomotion. Gait analysis has been employed clinically in stroke patients for their rehabilitation planning. In animal studies, gait analysis has been employed for the assessment of their locomotive disturbances in ischemic stroke, spinal cord injury and Parkinson's disease. The aims of the work reported here were to identify the gait parameters, collected from the computer-generated CatWalk System, that change after unilateral intracerebral hemorrhage (ICH) in the acute stage and long term up to 56 days post-ICH. The results showed that with the collagenase-induced unilateral striatal lesion, the rats displayed a significant contralateral decrease in print and maximum contact area and paw intensity, a diagonal increase in the stance duration of the left front and right hind paws, a significant decrease in the stride length of all four limbs, and foot pattern instability as reflected by the base of support, support on styles, and cadence. These deficits, including those in print area, stance and pressure, were demonstrated throughout the long-term period following ICH. The correlations between the gait parameters, lesion volume and asymmetrical forelimb use were also reported in this paper. This work has provided a systematic description on gait parameters in the classical striatal ICH model, which might become an essential assessment tool in future studies of pathophysiology and the development of novel treatments for experimental unilateral intracerebral hemorrhage with gait deficits.

© 2013 The Authors. Published by Elsevier B.V. Open access under CC BY-NC-ND license.

## 1. Introduction

Spontaneous intracerebral hemorrhage (ICH) is the most common stroke subtype. It is associated with a high mortality rate and only around half of all survivors are able to maintain independence [1,2]. ICH occurs in select locations of the brain, such as the basal ganglia, cerebellum, and brain stem, resulting in hematoma within the brain parenchyma that triggers a series of events leading to severe neurological deficits, including hemiplegia and hemidysesthesia. Its high rate of long-term disability and lack of pharmacological therapies make ICH one of the world's major health burdens. Many novel strategies that may benefit

* Corresponding author at: Division of Neurosurgery, Department of surgery, Prince of Wales Hospital, The Chinese University of Hong Kong, Hong Kong. Tel.: +852 2632 2624; fax: +852 2637 7974.
** Corresponding author at: Division of Neurosurgery, Department of surgery, Prince of Wales Hospital, The Chinese University of Hong Kong, Hong Kong. Tel.: +852 2632 2624.
*E-mail addresses:* lugang@surgery.cuhk.edu.hk (G. Lu), wpoon@surgery.cuhk.edu.hk (W.S. Poon).

0166-4328 © 2013 The Authors. Published by Elsevier B.V. Open access under CC BY-NC-ND license.
http://dx.doi.org/10.1016/j.bbr.2013.10.007

ICH patients have been explored in preclinical research, and several studies designed to mimic human ICH as closely as possible have been carried out to identify potential neuroprotective therapies. The development of appropriate animal models and sensitive evaluations of ICH motor deficits remains an active area of preclinical research into the effectiveness of therapeutic interventions [3,4].

A number of behavioral tests have been developed to determine the motor function outcomes of central nervous system (CNS) diseases in rodent models [5,6]. Existing tests to measure unilateral brain injury include the forelimb placing test, reaching test, cylinder test measuring forelimb use asymmetry, Modified Neurologic Severity Score (mNSS), and corner turn test [6,7]. These tests have been used for decades in studies of sensorimotor function following CNS injury. However, they suffer a number of limitations when used to assess unilateral dysfunction. For example, the forelimb placing test and mNSS require that rats be held by their torsos, while the cylinder test measures only forelimb use asymmetry, with the hind limbs neglected. Few studies have examined asymmetrical sensorimotor deficits in animals with unilateral ICH.

ICH patients may suffer a permanent loss of brain function or long-term deficits that take years to recover from. The main aim of preclinical research is to improve functional recovery in human beings. Most of the ICH animal models in current use are designed to mimic clinical situations. Although deficits may present close to ICH induction, animals that survive the initial ICH usually recover almost completely in approximately two months, with residual motor deficits minimally detectable using current investigative techniques [8,9]. Few studies have assessed functional impairments in long term. In a study using a collagenase model, the neurological deficit score had returned to normal in four weeks [10], and, in other studies, paw placement, cylinder, and ladder tests revealed impairment in one month after ICH [6,11,12]. The reaching test is effective for assessments in six weeks [13]. There is clearly a need for sensitive reproducible behavioral tests that can be used in experimental ICH research to assess the degree of damage and long-term residual impairment caused by unilateral CNS disorders and the process of recovery.

The CatWalk method is an automated, computerized gait analysis technique that allows objective quantification of multiple static and dynamic gait parameters. It has been used to assess gait in animal models of spinal cord injury [14], arthritis [15], pain [16], sciatic nerve injury [17], Parkinson's disease (PD) [18], and ischemic stroke [19], but not yet in animal models of ICH stroke. Hence, there is no experimental evidence concerning the CatWalk system's suitability for this particular application.

The aims of the work reported herein were thus to perform exploratory analysis of gait parameters to identify those that change in ICH rat models and to investigate the long-term deficits displayed by ICH rats using gait analysis. This work is the first to evaluate neurological disorders in ICH rat models using automated gait analysis.

## 2. Materials and methods

### 2.1. Animal preparation and intracerebral infusion

Our animal use protocols were approved by the Guide for the Animal Care and Use Committee of the Chinese University of Hong Kong. Forty adult male Sprague-Dawley rats (250–300 g) were used. All of the animals were housed under a 12 h light/12 h dark cycle with free access to food and water.

The rats were anesthetized with the intraperitoneal administration of 0.2 mL/100 g of a mixed solution containing 5 mg/mL of ketamine and 2.5 mg/mL of xylazine, and then secured prone onto

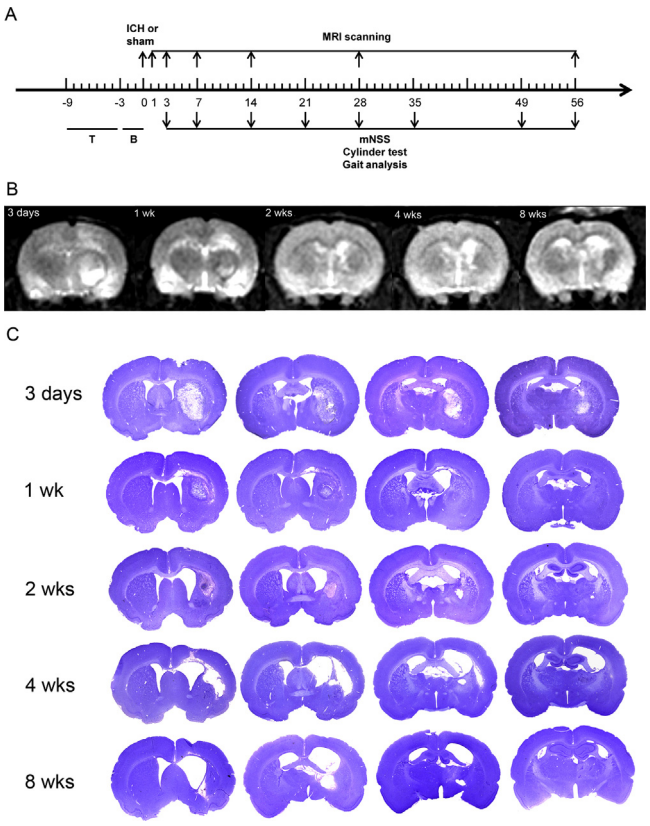


**Fig. 1.** (A) Schema illustrating the time course of testing procedures. Numbers indicate days relative to the ICH or sham surgery. T: training; B: baseline evaluations. (B) A representative images from MRI scanning at the level of maximum hematoma diameter on day 3, 7, 14, 28 and 56 following ICH. T2W1 of corresponding regions are shown. (C) A representative Nissl-stained image on day 3, 7, 14, 28 and 56 of the ICH rats with a cross section through the entire brain.

a stereotaxic frame before making an incision over the scalp. We then used the stereotactic coordinates to locate the striatum in the right hemisphere: 0.2 mm anterior, 3.0 mm lateral to the bregma and 6.0 mm deep. We drilled a 1-mm borehole, and then inserted a 26-gauge needle. Type IV collagenase (1.2 μL, Sigma, C5138 0.25 U in 1 μL NaCl 0.9%) was infused using a microinfusion pump. The syringe was left in place for 10 minutes before withdrawal to prevent back-leakage before being withdrawn. The borehole was then sealed with dental cement, the incision was closed, and the animals were kept warm and allowed to recover. The animals' body weights and the normality of their ambulation, feeding and grooming were the criteria used in assessing their wellbeing.

### 2.2. Neurological outcome measurements

Throughout the experiment, the animals were not subjected to any undue stress or irritation, and their condition and wellbeing were monitored. All of the behavioral training and testing (the protocols of which are described in the following paragraphs) were carried out in a quiet room at a fixed time during the animals' light phase by at least two experimenters who were blinded to experimental group. Baseline evaluations were conducted two days prior to surgery. Fig. 1A illustrates the time course of all neurological outcome measurements, with the time points of the testing procedures described in the figure legend.

#### 2.2.1. Modified neurologic severity scores (mNSS)

The mNSS was used to assess the neurologic deficits of the ICH rats from day 1 to day 56 [7,20]. The score is a composite of

motor, sensory (visual, tactile, and proprioceptive), balance, and reflex tests. Neurologic function is graded on a scale of 0–18, with 0 indicating normal neurologic function and 18 maximum functional deficit. In assessing injury severity, one point is awarded for the inability to perform a test or the lack of a tested reflex. Thus, the higher the score, the more severe the injury.

#### 2.2.2. Cylinder test

The forelimb use asymmetry test (cylinder test) was used to test spontaneous forelimb use from day 0 (pre-surgery) to day 56 [21]. Such use is sensitive to the damage caused by striatal ICH [12,22]. The rats were placed individually in a transparent cylinder (20 cm in diameter, 45 cm high) and videotaped from the side for 5 min using a mirror. The experimenters ensured that the entire cylinder was in view before recording. The initial placement of a forelimb on the wall and subsequent movements along the wall were counted as instances of spontaneous forelimb use. The percentage of affected limb use was calculated according to the following formula.

$$\frac{(\text{number of contacts with contralateral forelimb} + \tfrac{1}{2}\text{both}) \times 100}{\text{ipsilateral forelimb use} + \text{contralateral forelimb use} + \text{both}}$$

#### 2.2.3. Gait analysis: CatWalk data acquisition

The CatWalk method of gait analysis allows the easy quantitation of a large number of locomotion parameters. A full description of CatWalk analysis and the required training protocol can be found in Hamers et al. [23] and Koopmans et al. [24]. The CatWalk apparatus comprises a video and a meter-long glass plate with a fluorescent light beamed into the glass walkway floor from one side. As the rat walks along the walkway in a dimly lit environment, the light is reflected downward, and the animal's bright paw print images are captured by a video recorder mounted under the glass. The paw print footage is then analyzed automatically using the CatWalk computer program.

The animals received one-week of training prior to injury. They were familiarized with the walkway and trained to cross it for at least six times daily. Two criteria were used to ensure accurate locomotor analysis: (1) the rat needed to cross the walkway, without any interruption or hitch, and (2) a minimum of three correct crossings per animal were required [24]. As the rats were unable to perform a complete run on day 1 owing to weakness and stress, gait analysis was carried out on day 0 and then weekly from day 3 to day 56. A typical crossing contained six step cycles, and the data from all step cycles were averaged for analysis. The gait parameters of interest in the ICH model used in this work are as follows (LF = left forepaw; LH = left hind paw; RF = right forepaw; RH = right hind paw).

*Print area* ($mm^2$): The total floor area that comes into contact with the paw during the stance phase.

*Maximum contact* ($mm^2$): The paw area at the moment of maximal paw-floor contact during the stance phase. In contrast to the print area, for which gastrocnemius muscle paralysis was assessed, here but paw/toe dragging during part of the step cycle was measured [23].

*Duration of stance phase* (s): Because the duration of the stance or swing phase depends on the walking speed and degree of dysfunction, this parameter was transformed into a fraction of the total step duration: fraction stance = [stance duration/(stance duration + swing duration)] × 100%.

*Max contact mean intensity* (arbitrary unit [a.u.]): The mean pressure exerted by one individual paw in contact with the floor at the point of max contact.

*Base of support* (BOS, mm): The distance between two forepaws or two hind paws. The BOS is derived by measuring the distance (mm) between the mass-midpoints of the two forelimb prints or the two hind limb-prints at maximum contact.

*Duty cycle* (%): Stance as a percentage of step cycle (stance + swing):

$$\text{Duty cycle} = \frac{\text{stance}}{\text{stance} + \text{swing}} \times 100\%$$

*Stride length* (cm): The distance between successive placements of the same paw. It is based on the *X*-coordinates of the center of the paw print from two consecutive placements of the same paw during maximum contact.

*Support on* (%): The relative duration of simultaneous contact with the floor by all combinations of paws: zero paws, a single paw, a diagonal pair of paws (RF-LH or LF-RH), girdle paws (RF-LF or RH-LH), three paws, and four paws.

*Cadence* (steps/s): Cadence is expressed in steps per second:

$$\text{Cadence} = \frac{\text{step-1}}{\text{initial contact last stance} - \text{initial contact first stance}}.$$

#### 2.2.4. Magnetic resonance imaging (MRI)

MRI was performed on days 0–56 on a 3-T clinical scanner (Achieva, Philips Healthcare, Best, The Netherlands). After anesthesia administration, the rats were placed in the prone position, and a custom-made quadrature RF volume coil (internal diameter = 7 cm) was used as the signal transmitter and receiver. A three-plane coronal-sagittal localizing spin-echo sequence was first used to identify the position of the brain. Then, 13 contiguous coronal T2-weighted images were used to cover the whole rat brain. The parameters for the T2-weighted imaging were 2D turbo spin echo (TSE) sequences with TSE factor = 10, echo delay time/repetition time (TE/TR) = 100 ms/2000 ms, field of view (FOV) = 40 mm × 40 mm × 28 mm, acquisition matrix = 132 × 133, voxel size = 0.3 mm × 0.3 mm × 2 mm, the number of signal averages (NSA) = 3, slice thickness = 2.0 mm, and slice gap = 0.2 mm. Four slices were used to evaluate the hematoma and volume of injury, and the images were analyzed with a Philips DICOM Viewer. The volume of tissue loss was calculated using the following equations [12].

Volume of tissue loss

= remaining volume of non-injured hemisphere

−remaining volume of injured hemisphere;

Volume of hemisphere

= average(area of coronal section of the hemisphere

−area of ventricle − area of damage)

×section interval × number of sections.

#### 2.2.5. Histology and volumetry

At 3, 7, 14, 28, 42, and 56 days after ICH, the rats were transcardially perfused with 0.9% saline followed by 4% paraformaldehyde (PFA) in phosphate buffered saline (PBS). Their brains were then removed, fixed in 4% PFA, and dehydrated in 15%, 20%, and finally, 30% sucrose. Forty micrometer cryostat processed tissue sections were taken every 200 μm through the entire brain and stained with cresyl violet. Histological analysis was performed by a researcher who was blinded to the treatment condition. Volume of tissue loss was calculated using the Spot Imaging System and the following equations [12].

Volume of tissue loss = remaining volume of normal hemisphere

− remaining volume of injured hemisphere;

Volume of hemisphere = average(area of complete coronal section of the hemisphere − area of ventricle − area of damage) × interval between sections × number of sections.

### 2.3. Statistical analysis

All data presented herein is in the form of mean ± standard error of the mean. All of the behavioral tests were carried out by at least two experimenters who were blinded to group identity. The behavioral scores for the cylinder test and mNSS were analyzed using repeated-measures analysis of variance (ANOVA) (SPSS 17.0; SPSS Inc., Chicago, IL, USA), followed by one-way ANOVAs (print area, maximum area, stance, pressure, duty cycle, average speed, cylinder test, body weight) or the Mann–Whitney U test (mNSS score, LF/RF swing, LH/RH swing speed, stride length, BOS, cadence, support on styles) to analyze the differences between the ICH and sham rats at a given time point. Pearson's correlation coefficients were calculated to determine the relationship between functional impairment and CatWalk outcome. Finally, linear regression was performed to determine the equation of the relationship. Grubbs' outlier detection procedure was performed to detect the outliers. A $p$-value of 0.05 was considered the threshold for a significant difference.

## 3. Results

### 3.1. Lesion imagines via MRI scanning and histology sections

All animals ($n = 6$ at each time point) in the experimental group demonstrated a sizable ICH region, with a maximum tissue loss volume on day 1. Fig. 1B shows the MRI images at the maximum hematoma diameter level at each scan time on day 3, 7, 14, 28 and 56. Hematoma formation began on day 1, and increased until it reached its peak volume on day 3. Most of the hematoma had been absorbed one-month post ICH and its eventual resolution resulted in a cavity, and commonly ventriculomegaly, between one and two months. The tissue loss volume in ICH group ($n = 6$) was greatest on day 1 ($79.17 \pm 2.68\ mm^3$), ($73.81 \pm 1.45\ mm^3$) on day 3 and changed over time (one-way ANOVA, $p < 0.0005$). In the first month after ICH, tissue loss volume decreased in line with hematoma resolution, and on day 28 the volume was reduced to nearly one-quarter of day 1 ($25.71 \pm 2.05\ mm^3$, $p < 0.0005$). After one month, the tissue loss volume increased in line with cavity formation and ventricular enlargement, reaching $36.11 \pm 2.48\ mm^3$ on day 56. Edema and the mass effect of the hematoma were apparent before the end of the first week, with the volume of tissue loss increasing markedly between one and four weeks, similar to those results described in MacLellan et al. [10].

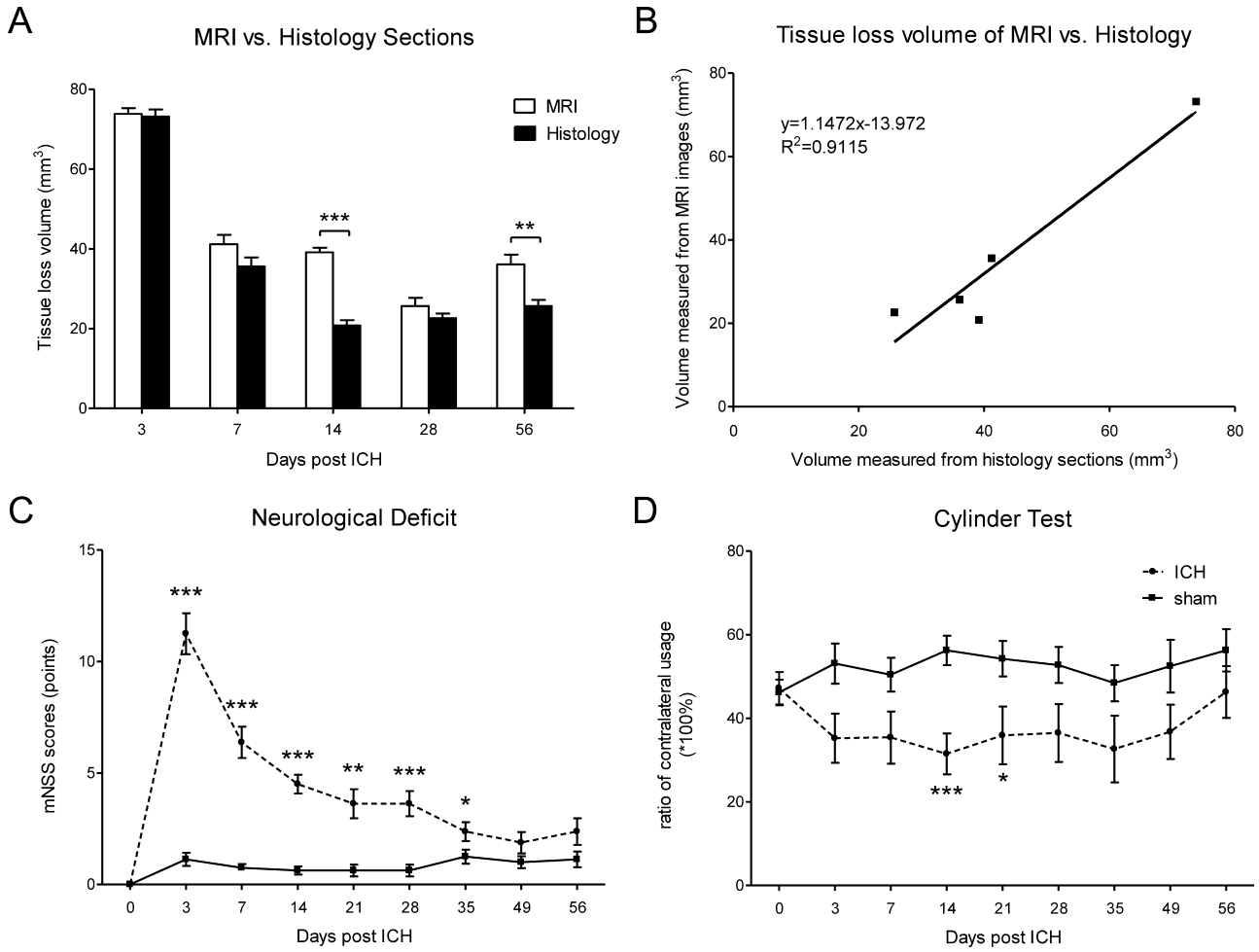


**Fig. 2.** (A) Comparison of the tissue loss volume as calculated from MRI scanning and Nissl-stained histology sections. (B) Regression analysis revealed a significant correlation between tissue loss volume measurements obtained from MRI scanning and histology sections. (C) mNSS score of rats in the ICH and sham groups. (D) Cylinder test (forelimb asymmetry use) shown as the percentage of wall contacts made with the contralateral forelimb in ICH and sham groups ($n = 10$ in each group), data are shown as mean ± SEM. $^{***}p < 0.001$, $^{**}p < 0.01$, $^{*}p < 0.05$.

Consistent with the MRI images, the Nissl-stained sections of ICH rats ($n = 6$ at each time point) showed collagenase injection result in hematoma formation, with extensive injury to the right striatum (Fig. 1C). Beyond what the MRI images indicated, these sections also showed that the anterior regions of the caudate nucleus and ipsilateral corpus callosum were damaged along the tract, with the injured tract terminating near the external globus pallidus and even the internal capsule. White matter damage was found in the corpus callosum one week after ICH and in the internal capsule two weeks after. The resultant tissue loss volumes were measured and correlated with the MRI images (Fig. 2A). Quantitative measurement demonstrated a volume of $73.18 \pm 1.77\,mm^3$ with the hematoma and edema on day 3 and of $35.59 \pm 2.30\,mm^3$ with the resolved hematoma and enlarged lateral ventricles on day 7. The tissue loss volumes measured from the Nissl-stained sections were significantly smaller than those measured from the MRI images on day 14 ($p < 0.0005$) and day 56 ($p = 0.005$). Regression analysis revealed a significant correlation between the volume measurements obtained from the MRI images and those obtained from the histology sections ($R^2 = 0.9115$, $p < 0.005$; Fig. 2B).

### 3.2. Effect of ICH on mNSS scores

In the mNSS analysis (Fig. 2C), all animals ($n = 10$ in each group) showed a significant neurologic dysfunction from day 3 to day 35, and with a highest scores of $11.25 \pm 0.92$ on day 3 ($p < 0.01$).

### 3.3. Effect of ICH on cylinder test scores

The test affected contralateral forelimb use during wall exploration revealed there to be no time effect ($p = 0.879$) or time × group effect ($p = 0.332$), but a significant group effect at all times ($p = 0.018$). The ICH groups ($n = 10$ in each group) used their contralateral forelimbs less often than the sham groups ($p = 0.005$, Fig. 2D), with the significant differences found on day 14 ($p < 0.001$), and day 21 ($p < 0.05$).

### 3.4. Effect of ICH on CatWalk gait -analysis

The CatWalk system captures a substantial number of gait parameters, both dynamic and static (Fig. 3A). Some static parameters, such as paw *mean intensity*, paw *print area*, and *maximum paw contact area*, are defined as individual paw parameters, which depended on the animal's body weight [25]. Others, such as *stride length* and *BOS*, indicate motor coordination when used to measure the distance between two paws (Fig. 3A), and are thus less dependent on weight or speed. Most of the gait parameters, including *stance* and *swing*, are strongly speed-related [26,27]. Hence, the related parameters were transformed into the ratio between the contralateral and ipsilateral sides (LF/RF and LH/RH) to (1) adjust for confounding factors and (2) to identify the hemiplegic gait asymmetry after unilateral ICH injury.

The mNSS assessment of the rats' post-ICH neurological outcomes revealed that the most severe deficits occurred from day 1 to day 3. Accordingly, we compared the gait parameters of the ICH and sham groups ($n = 10$ in each group) on day 3 to identify the impaired gait parameters. An explanatory overview of these parameters is provided in Table 1. Statistical analysis showed the unilateral ICH rats had experienced significant impairment on day 3 in *print area*, *maximum contact area*, fore paw *stance*, *pressure*, *swing speed*, hind paw *duty cycle*, *stride length*, fore paw *BOS*, *support on style* (three limb-support), *cadence* and *average speed*. A brief overview of the injured print and gait patterns is presented in Fig. 3B, and the affected gait parameters are summarized in Fig. 3C. The most significant parameters analyzed using CatWalk are described in further detail in the following paragraphs.

#### 3.4.1. A contralateral decrease in print area in the LF and LH was related to tissue loss volume, mNSS scores, and contralateral limb use deficit

The print area derived from the automatic boxes that the CatWalk software places in every frame around the single paw print revealed an unequal distribution of the two front paws and two hind paws (Fig. 4A and B). After ICH injury, the *print area related to* paw size was reduced by nearly 20% (Fig. 4A, $p < 0.001$) in the contralateral paws (LF and LH) on day 3, with the deficits lasting for about two months. Those derived from the injured front paw prints showed a gradual recovery process, although tending to remain below 100% on day 56 (Fig. 4A, $p < 0.001$). The *print area* of the injured left hind paw was reduced to about 80% on day 3, increasing to 92% on day 49 (Fig. 4B, $p < 0.01$). Significant correlations were found between mNSS scores (Fig. 4C; $R^2 = 0.7981$, $p < 0.05$), contralateral limb use (Fig. 4D, $R^2 = 0.6031$, $p < 0.05$), tissue loss volume obtained from both the MRI images (Fig. 4E, $R^2 = 0.9714$, $p < 0.05$) and histology sections (Fig. 4F, $R^2 = 0.8640$, $p < 0.05$), and the decreased *print area* after striatal ICH injury.

#### 3.4.2. Diagonal increase in stance duration in the LF and RH

The timing of paw placement was detectable in the stance phase indicated by the colored tags in Fig. 5A and B. The vertical colored bars showed the more regular pattern observed in the normal rats and the relative time increase in the left front and right hind paws. Our data showed the value of the dynamic parameter of *stance* phase to have been strongly affected by walking speed. The timing of the four paws *stance* increased significantly on day 3, given the decrease in walking speed. However, the ratio between the contralateral (left) and ipsilateral (right) paws exhibited an opposite tend in the front and hind paws. The *stance* phase of the contralateral front paw (LF) in response to the ICH injury increased to 110% of the ipsilateral front paw (RF) on day 3 (Fig. 5A, $p < 0.001$). The value of contralateral hind paw (LH) was reduced to 97% on day 3 (Fig. 5B, $p < 0.01$). A significant difference was found on day 28 in fore paw (Fig. 5A, $p < 0.05$), and on day 35 in the hind paw (Fig. 5B, $p < 0.01$).

#### 3.4.3. Contralateral decrease in pressure in the LF and LH

This parameter *pressure* measures the mean intensity at the maximum paw contact area (MeanIntensity at Maximum contact, a.u.) during running of individual paw. The *pressure* of contralateral paws (both fore and hind paws) decreased compared with the ipsilateral paws on day 3 after ICH (Fig. 5C and D). When compared with the ipsilateral paws, 5% decrease of *LF pressure* was found on day 3 and 2% decrease on day 56 (Fig. 5C, $p < 0.001$). In hind limbs, 4% decrease of *LH pressure* could be found on day 3 (Fig. 5D, $p < 0.01$), the trend lasted until day 49 ($p < 0.01$).

#### 3.4.4. Average speed and body weight

An animal's body weight and speed in crossing the walkway can influence several parameters. Therefore, group comparison ($n = 10$ in each group) was performed to determine whether there were any differences in the weight and speed of the two groups at a given time point (Fig. 5E and F). On day 3, 7, 21 and 28, there were significant differences of *average speed* in two groups (Fig. 5E, $p < 0.05$). On day 7, there were significant differences of body weight in two groups (Fig. 5F, $p < 0.05$). Thus if the individual paw parameters were not adjusted by transforming equations, the data would be strongly influenced by body weight and *average speed*. The coordination parameters like *stride length*, *base of support* and *support on*

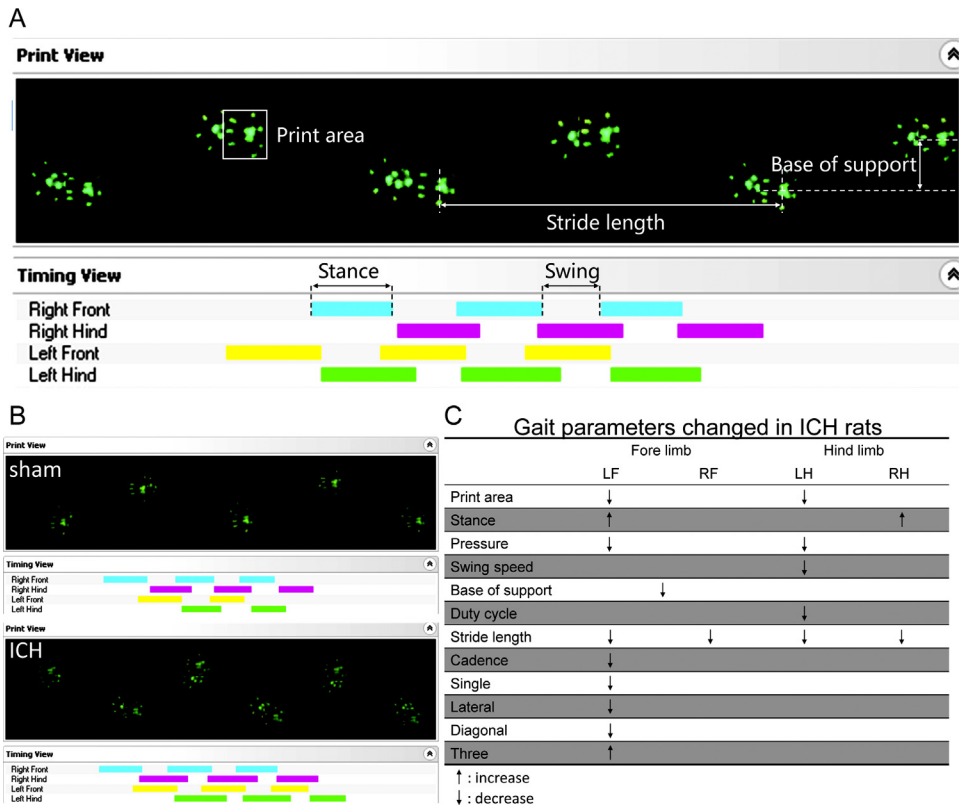


**Fig. 3.** (A) Graphical representation of gait parameters. (B) Two walking patterns collected 3-days post-ICH or sham surgery. The upper panel (green prints in black background) shows the digitized prints, while the lower panel (with colorful phase lags) shows the stance phase duration of each individual paw in a single step cycle. blue, RF; red, RH; yellow, LF; green, LH. (C) Gait parameters of the ICH versus sham groups. (For interpretation of the references to color in this figure legend, the reader is referred to the web version of the article.)

*styles* were related to the foot patterns and not affected by weight and speed.

#### 3.4.5. Decrease in stride length in all four limbs

The stride length (referred to as step length in human beings) of the right striatum - injured rats was significantly shorter than that of the sham group in all four limbs (Fig. 6) on day 3 (all $p < 0.001$). The decreased *stride length* of LH and RH persisted throughout the first two weeks after ICH (Fig. 6B and D; $p < 0.001$), the decreased *stride length* of LF was detected on days 3 and 7 (Fig. 6A, $p < 0.001$), and the decreased *stride length* of RF was detected on day 28 (Fig. 6C, $p < 0.001$).

#### 3.4.6. Lack of trunk stability detected from the variation in BOS, support on style and cadence

Compared with sham group, the *forelimb-BOS* of ICH rats was shorter with significant difference (Fig. 6E, $p < 0.01$), the *hindlimb-BOS* was shorter without statistical significance (Fig. 6E, $p > 0.05$). Significant differences in *Support On Style* were found between the ICH and sham groups on day 3 (Fig. 6F), when the ICH rats displayed more frequent occurrences of three- and four-paw-combinations, and less frequent occurrences of single, lateral, girdle and diagonal paw use ($p < 0.05$). *The cadence* of ICH rats underwent a significant reduction on day 3, falling to 80% of that of the sham rats (Table 1, $p < 0.01$).

## 4. Discussion

This work constitutes the first use of the CatWalk system, an automated gait analysis tool, to measure locomotion deficits in rat models of ICH stroke. Previous studies have reported gait impairment in unilateral middle cerebral artery occlusion (MCAO) [3,28], pyramidotomy lesion [29], cervical spinal cord contusion [30], and PD [3] models. More specifically, they have reported gait impairment in *print area*, *stride length*, *swing speed*, and coordination of injury. The longest lasting effects were observed in contralateral paw *intensity*, which lasted for 3 weeks after 6-OHDA was injected into the unilateral basal ganglia [3], and in *stride length*, which lasted for 28 days after a cutting injury to the medulla fibers [29].

### 4.1. Long-term assessment of gait parameters in ICH rat model

In the work reported herein, we found short-term deficit recovery within 1 month of ICH, including recovery in *maximum area*, *duty cycle*, *stride length*, *front paws BOS*, *support on styles* and *cadence*. Longer-lasting deficits (up to 2 months) were observed in *print area*, *stance phase duration*, and *pressure*.

Print area on the walkway is directly related to pressure, and indicates the relative force exerted during locomotion [16]. The results of our gait analysis revealed that rats with unilateral ICH lesions in the right striatum exhibit reduced contralateral paw *print areas* and contralateral limbs weight-bearing. An asymmetrical *print area* was observed between the contralateral and ipsilateral paws. A 20% decrease in impaired contralateral front paws (LF) and hind paws (LH) were observed on the third following ICH. Such impairment lasted for 2 months in fore paws and 49 days in hind paws. This discrepancy is most likely due to compensation by the animal, that is, it spares the affected paw by allowing the non-injured paw to bear more weight. Our data suggest that, *print area* asymmetry is a reliable parameter for use in long-term studies of ICH rodent models.

**Table 1**
CatWalk parameter statistics for measuring ICH neurological deficits post-ICH.

| | | Mean | Std. error | *F* | Sig. |
|---|---|---|---|---|---|
| Print area LF/RF | ICH | .844 | .020 | 19.400 | .000*** |
| | Sham | 1.003 | .020 | | |
| Max area LF/RF | ICH | .849 | .030 | 12.002 | .001** |
| | Sham | .997 | .024 | | |
| Stance LF/RF | ICH | 1.103 | .033 | 11.063 | .001** |
| | Sham | 1.021 | .009 | | |
| Pressure LF/RF | ICH | .954 | .008 | 12.898 | .000*** |
| | Sham | .986 | .005 | | |
| Print area LH/RH | ICH | .813 | .032 | 22.096 | .000*** |
| | Sham | 1.008 | .025 | | |
| Max area LH/RH | ICH | .847 | .040 | 13.428 | .000*** |
| | Sham | 1.135 | .046 | | |
| Stance LH/RH | ICH | .972 | .016 | 2.254 | .136 |
| | Sham | 1.008 | .023 | | |
| Pressure LH/RH | ICH | .961 | .012 | 11.010 | .001** |
| | Sham | 1.003 | .006 | | |
| Swing LF/RF | ICH | .907 | .035 | 13.903 | .000*** |
| | Sham | 1.016 | .012 | | |
| Swing LH/RH | ICH | 1.135 | .036 | 14.595 | .000*** |
| | Sham | 1.016 | .014 | | |
| Swing speed LF/RF | ICH | 1.168 | .069 | 8.703 | .004** |
| | Sham | 1.034 | .012 | | |
| Swing speed LH/RH | ICH | .901 | .024 | 23.912 | .000*** |
| | Sham | 1.014 | .011 | | |
| Duty cycle LF/RF | ICH | 1.034 | .012 | .035 | .852 |
| | Sham | 1.020 | .013 | | |
| Duty cycle LH/RH | ICH | .984 | .009 | 6.077 | .015* |
| | Sham | 1.015 | .008 | | |
| Stride length (LF, cm) | ICH | 14.720 | .278 | 18.908 | .000*** |
| | Sham | 16.294 | .191 | | |
| Stride length (LH, cm) | ICH | 13.985 | .289 | 45.935 | .000*** |
| | Sham | 16.095 | .158 | | |
| Stride length (RF, cm) | ICH | 14.635 | .283 | 18.547 | .000** |
| | Sham | 16.319 | .209 | | |
| Stride length (RH, cm) | ICH | 14.649 | .305 | 36.467 | .000** |
| | Sham | 16.414 | .139 | | |
| BOS_Front (mm) | ICH | 2.448 | .068 | 10.141 | .002** |
| | Sham | 2.715 | .045 | | |
| BOS_Hind (mm) | ICH | 3.667 | .142 | 1.362 | .246 |
| | Sham | 3.843 | .075 | | |
| Support on single (%) | ICH | .000 | .000 | 1.197 | .278 |
| | Sham | .108 | .108 | | |
| Lateral (%) | ICH | .127 | .075 | 3.192 | .079 |
| | Sham | .873 | .448 | | |
| Diagonal (%) | ICH | .802 | .350 | 3.523 | .065 |
| | Sham | 3.408 | 1.460 | | |
| Three (%) | ICH | 4.192 | .988 | 4.508 | .037* |
| | Sham | 1.709 | .490 | | |
| Four (%) | ICH | 43.867 | 2.069 | 2.374 | .128 |
| | Sham | 38.844 | 2.567 | | |
| Cadence (steps/s) | ICH | 8.220 | .186 | 8.033 | .005** |
| | Sham | 10.340 | .210 | | |
| Average Speed (mm/s) | ICH | 28.272 | 1.692 | 61.432 | .000*** |
| | Sham | 44.265 | 1.076 | | |

* $p < 0.05$.
** $p < 0.01$.
*** $p < 0.001$.

After ICH injury, the duration of *stance* phase increased significantly in the diagonal pair, LF and RH, and decreased in LH and its coupled RF. Previous studies of CNS disorders have failed to investigate this parameter. In researches using mechanical allodynia and inflammatory pain rat models, the *stance* phase was shorter in the neuropathic paw [16,31]. In our study, however, the diagonal pairs of LF/RH revealed an increasing *stance* phase relative to RF/LH. We observed a nearly 5% increase in LF versus RF and 5% decrease in LH versus RH. An explanation for these apparent asymmetries is weight loading compensation in RH and limb-dragging in LF, in addition to the rats' failure to flex their limbs adequately during the swing phase.

As described in previous studies [3,32,33], paw *pressure* was measured as light intensity, which is the mean intensity of all pixels of the print at the point of max contact. It was a measure of pressure and weight support exerted by single paw on the glass plate during locomotion. In photothrombotic stroke, PD and monoarthritis models, the injured paw *pressures* were significantly reduced [3,33] because of weight-bearing change. In current work, when comparing contralateral and ipsilateral, a 5% reduction was observed in LF and LH. Significant and long-lasting changes were found in both fore and hind paws, thus suggesting that the animals exerted more force with the non-impaired paw (RF and RH) following ICH.

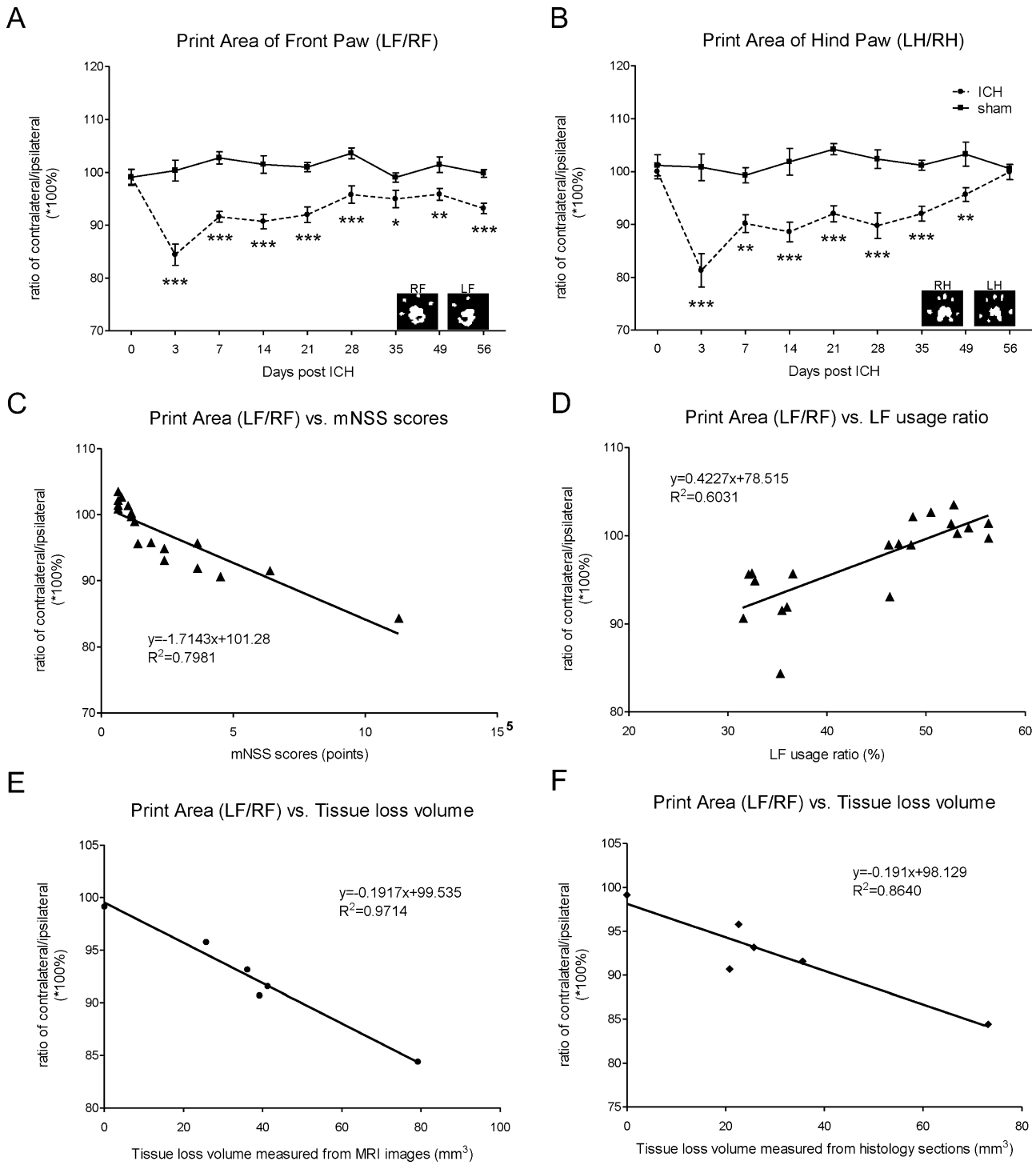


**Fig. 4.** Gait parameter print area measurements obtained from CatWalk system during a 56-day observation following ICH and sham operation ($n = 10$ in each group). Print area in contralateral front paw (LF) decreased in ICH rats (A) and print area in contralateral hind paw (LH) decreased in ICH rats (B). Data are shown as mean ± SEM. $^{***}p < 0.001$, $^{**}p < 0.01$, $^{*}p < 0.05$, compared with sham group at the same time point value. Regression analysis revealed (C) a significant correlation between decreased LF paw print area and mNSS score ($R^2 = 0.7981$, $p < 0.05$); (D) a significant correlation between decreased LF paw print area and LF use ratio ($R^2 = 0.6031$, $p < 0.05$); (E) a significant correlation between decreased LF paw print area and lesion volume measurements obtained from MRI images ($R^2 = 0.9714$, $p < 0.01$); (F) a significant correlation between decreased LF paw print area and lesion volume measurements obtained from histology sections ($R^2 = 0.8640$, $p < 0.01$).

### *4.2. To eliminate the confound effects of running speed and body weight in gait parameters*

In many previous animal studies of gait analysis, including those of peripheral nervous system fiber degeneration animal models (such as sciatic nerve injury) and CNS disorders (such as PD and olivocerebellar degeneration), static parameters such as *mean intensity* and *print area* may have been be strongly affected by body weight. Whereas, dynamic parameters such as *stance* duration, *swing* duration and *duty cycle* are not only involved the motor control of the animal, but also have been linked to neuropathic pain [16], locomotion speed and body weight [17,27]. For a reliable comparison of the gait parameters of animals in the impaired group and sham group, it is important to ensure that there is no

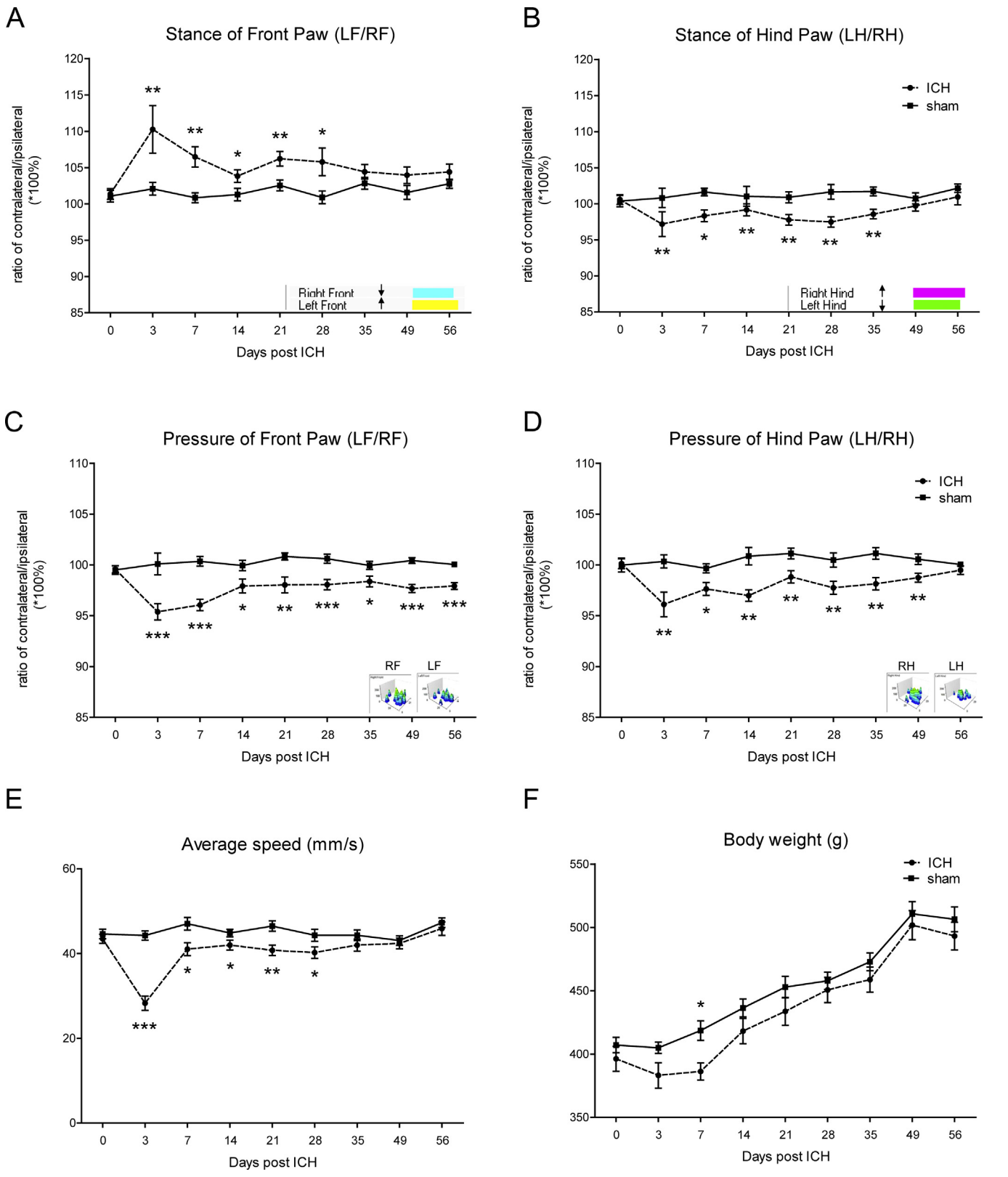


**Fig. 5.** Gait parameters measurements obtained from CatWalk system during a 56-day observation following ICH and sham operation ($n = 10$ in each group). Stance phase duration in contralateral front paw (LF) decreased in ICH rats (A) and stance phase duration in contralateral hind paw (LH) increased in ICH rats (B). Pressure in contralateral front paw (LF) (C) and in contralateral hind paw (LH) (D) decreased in ICH rats. The-time course changes in the average speed (E) and animals' body weight (F) within 56-day of observation. Data are shown as mean ± SEM. $^{***}p < 0.001$, $^{**}p < 0.01$, $^{*}p < 0.05$.

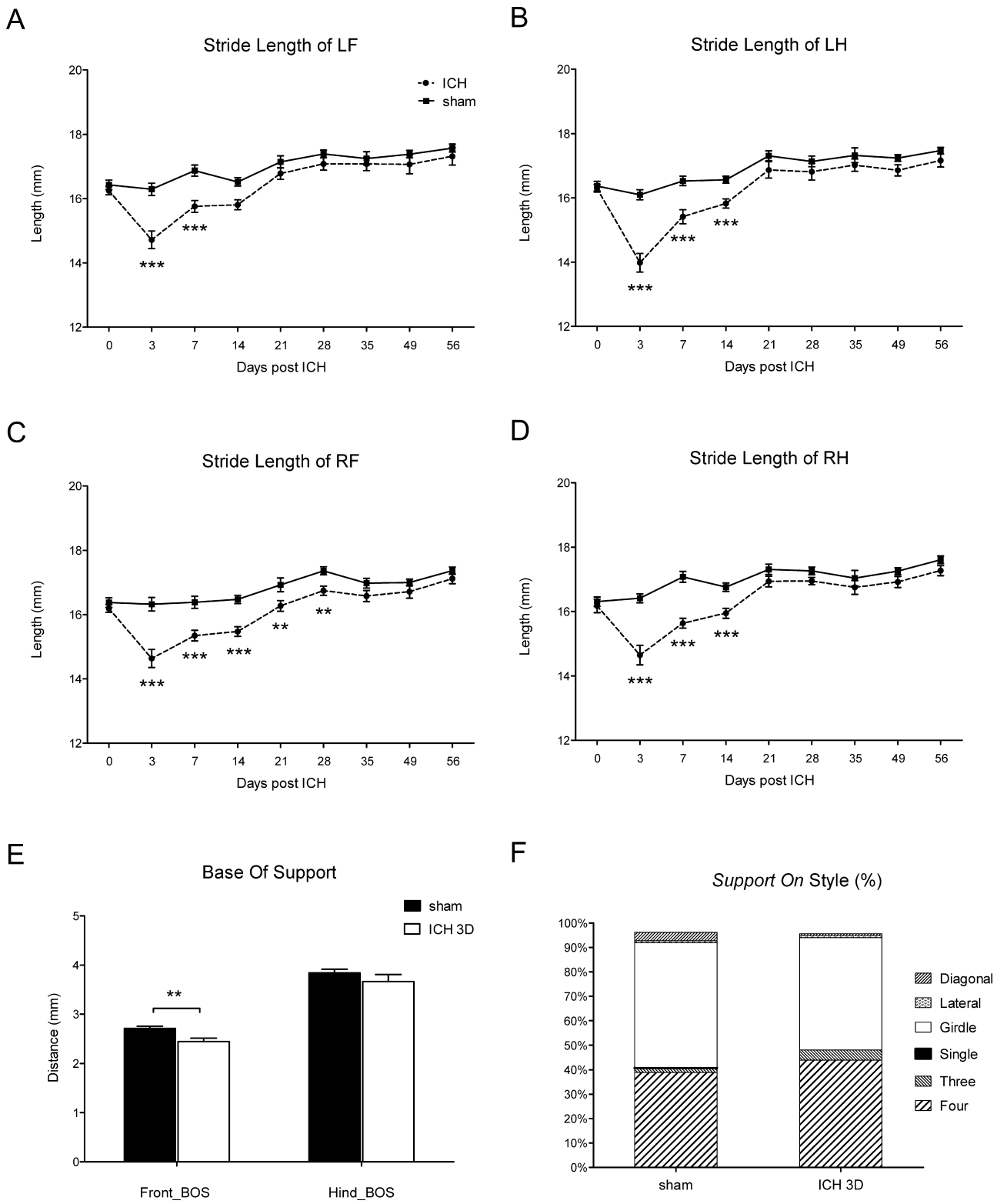


**Fig. 6.** Gait parameter stride length measurements obtained from CatWalk system during a 56-day observation following ICH and sham operation ($n = 10$ in each group). Stride length in all four limbs (A–D) decreased in ICH rats. BOS in both front and hind paws (E) decreased in ICH rats. The percentage of support on styles decreased in single-, diagonal-, girdle- and lateral patterns in ICH rats, and increased in three- and four-patterns. (F). Data are shown as mean ± SEM. $^{***}p < 0.001$, $^{**}p < 0.01$, $^{*}p < 0.05$, compared with sham group at the same time point value.

difference in gait speed or body weight between the two groups [24]. Hence, to eliminate any discrepancies in our interpretation of running speed and to ensure that the baseline ran duration held relatively constant at 1.0–2.5 s for all rats, all of the animals were forced to run twice per day during the seven-day-training period. Further, to prevent the effects of speed and weight confounding the gait parameter results, the non-impaired ipsilateral paws were always taken as the control for the affected paws.

### 4.3. Coordination-related parameters in ICH rat model

*Base of support* (*BOS*) is a coordination-related parameter. The farther apart the feet are placed during locomotion, the less likely the animal is to fall and the larger the *BOS* [34]. Previous studies of rats with olivocerebellar degeneration [27], pyramidotomy lesion[29], PD [32], cervical spinal cord injury [33], midthoracic spine contusion [35] and arthritis [36] have used hind paw *BOS* as a coordination parameter to assess treatment outcome. Hind paw *BOS* was wider in olivocerebellar degeneration and spinal cord injury models [27,37,38]. Fore paw *BOS* was smaller in PD model (bilateral 6-OHDA lesions). No significant difference was found in unilateral pyramidotomy lesion model [29]. In this current study, a decrease in the *BOS* of both the front and hind paws was seen on day 3. The reduced forelimb base of support displayed an effect of the lesion in the interlimb placement of the forepaw, which was also observed in PD lesion rats in previous study [32]. In research on gait of humans, the *BOS* was significantly reduced due to impairment of lateral foot placement following a neurological disease or brain trauma [39]. Reduced *BOS* during walking may consequently lead to postural instability. Hip flexion lost, pelvic retraction and asymmetry in hemiplegia were considered to be the primary causes of narrow *BOS* [40,41].

In research on human hemiplegic gait, the step lengths (*stride lengths*) of subjects with stroke were shorter than those of healthy elderly subjects [37]. Weakness in the affected hip flexors and the spasticity of the affected ankle plantarflexors may contribute to step length deficits [38]. In a rat unilateral pyramidotomy lesion model [29], cervical contusion model [23] and PD model [42], a significant decrease in stride length was observed after injury, although these studies did not report the parameter's time trend. In this current study, stride length was reduced by approximately 30% in all limbs, a similar result to that found in a clinical study [43]. As diagonal paired limbs (e.g., RF-LH and LF-RH) are coordinated when rats run, the stride length of all four limbs displayed the same decreasing trend, with no asymmetry found between the left and right limbs, although the asymmetrical step length in right and left has been observed in stroke patients [38]. In analysis of stride length, the effects of increasing body weight and body length should also be taken into consideration.

Our measure of limb support comprised single, double, triple and quadruple limb use. Our results suggested that rats with ICH lesions rely more for support on the use of three or four limbs when running than on double limb use (diagonal and lateral), possibly to compensate for trunk instability. Cadence was shorter in stroke patients than healthy controls in a previous study [37], which accords with our observation of ICH rats, exhibiting 20% reduction in cadence relative to their sham counterparts. The difference is possibly due to a lack of balance and the spasticity or contracture of the affected plantar flexors.

In our study, the same results were observed in ICH rats, in which a 30% reduce was found in comparison of sham rats. It is possibly due to the unbalance in moving body over an unstable leg, and spasticity or contracture of the affected plantarflexors.

### 4.4. Tissue loss measured by using MRI and histology sections

As expected from the functional location of the hematoma in the right striatum, which was confirmed by the MRI T2 images, the ICH rats displayed a sensorimotor function deficit in the left fore/hind limbs, as measured by the mNSS, and impairment in left fore-limb use, as measured by the cylinder test. Gait analysis demonstrated significant differences in print area and intensity between the contralateral and ipsilateral forelimbs.

The equations used to calculate tissue loss volume showed that in the acute phase of ICH, such volume consists primarily of hematoma expansion and edema. In the delayed phase that follows edema recession and hematoma reabsorption, in contrast, tissue loss volume consists mainly of the lesion volume (such as cavity and cellular debris) and ventricular enlargement resulting from neuronal death and white matter loss. We hypothesized that that the greater tissue loss volume in the unilateral striatum may contribute to the greater impairment seen in the sensorimotor function of contralateral limb use and affected paw print area. Our results supported this hypothesis, as they reveal a significantly positive correlation between print area asymmetry and MRI tissue loss volume ($R^2 = 0.971$), histology tissue loss volume ($R^2 = 0.864$), mNSS score ($R^2 = 0.798$), and contralateral limb use ($R^2 = 0.603$). The implication is that brain tissue loss and sensorimotor deficits may contribute to an asymmetrical decrease in affected limb use and print area.

Although T2-weighted MRI images are better at identifying the effects of hemoglobin degeneration and changes in tissue water (edema) in the early stages of ICH [44], the measurements of hematoma volume or tissue loss were easily confounded by the mass effect of the hematoma and edema. Due to the slice thickness limitation of 3 T MRI (2.0 mm), the tissue loss volume would be overestimated by using MRI compared with histology sections (0.03 mm) [10]. Compared with the images obtained from 3T MRI, the Nissl-stained sections exhibited a more clearly anatomical definition of the striatum, hippocampus, and white matter structures, including the internal capsule and corpus callosum. Histology sections are more reliable for identification of white matter injury one week after ICH. The limitation of histology sections is that brain shrinkage occurs during fixation and dehydration, which may lead to the previously reported discrepancy in tissue loss volume measured on days 14 and 56 using MRI images and histology sections [45]. Similar to the results obtained from a 7T-MRI scanner in an earlier study [44], we also found a strong correlation between MRI images and histology sections in measuring post-ICH tissue loss volume. However, histology sections were irreplaceable in the exact quantification of white matter damage and tissue loss in ICH.

## 5. Summary

No single animal behavioral test is capable of revealing all of the neurological deficits resulting from ICH. Furthermore, given the differences between rodents and human beings, the translation of preclinical findings using animal models to the clinical arena requires caution. Such translation may be facilitated, however, by improved animal models and well-designed investigative techniques. Preclinical research aimed at finding interventions that benefit functional outcomes is best served by animal models and assessments that closely mimic the course of human disease. The collagenase-striatum induction model mirrors the hematoma growth and hemiplegia seen in human ICH. Further, gait analysis reveals the asymmetrical contralateral limb gait pattern and trunk instability that follows ICH in humans. Gait analysis may also be useful in studies of long-term sensorimotor deficits in rodent ICH models. Advanced investigations of the relationship between gait parameters and hemiplegia, spasticity, and sensory disturbance are still needed.

## 6. Conclusion

We have developed a reproducible and consistent ICH model for of unilateral CNS sensorimotor disorder in rat. We have demonstrated that gait analysis by CatWalk system is a useful tool of measuring locomotion deficits following ICH by showing detailed impairment of each individual paw and overall gait pattern. We

have found out several gait parameters that could be used to evaluate related long-term deficits of experimental rat ICH model. Gait analysis will provide a valuable method for assessing therapeutic strategies to promote fiber regeneration following stroke.

## Acknowledgements

The study was supported by a great (No. RGC-473709) from the Research Grants Council of Hong Kong, a direct grant from the Chinese University of Hong Kong (No. CUHK-2041730) and a grant from National Natural Science Foundation of China (No. 81271393). We would like to thank the anonymous reviewers for their constructive comments.

## Appendix A. Supplementary data

Supplementary data associated with this article can be found, in the online version, at http://dx.doi.org/10.1016/j.bbr.2013.10.007.

## References

[1] Feigin VL, Lawes CM, Bennett DA, Barker-Collo SL, Parag V. Worldwide stroke incidence and early case fatality reported in 56 population-based studies: a systematic review. Lancet Neurol 2009;8:355–69.
[2] van Asch CJ, Luitse MJ, Rinkel GJ, van der Tweel I, Algra A, Klijn CJ. Incidence, case fatality, and functional outcome of intracerebral haemorrhage over time, according to age, sex, and ethnic origin: a systematic review and meta-analysis. Lancet Neurol 2010;9:167–76.
[3] Vandeputte C, Taymans JM, Casteels C, Coun F, Ni Y, Van Laere K, et al. Automated quantitative gait analysis in animal models of movement disorders. BMC Neurosci 2010;11:92.
[4] Fisher M, Feuerstein G, Howells DW, Hurn PD, Kent TA, Savitz SI, et al. Update of the stroke therapy academic industry roundtable preclinical recommendations. Stroke 2009;40:2244–50.
[5] Belayev L, Saul I, Curbelo K, Busto R, Belayev A, Zhang Y, et al. Experimental intracerebral hemorrhage in the mouse: histological, behavioral, and hemodynamic characterization of a double-injection model. Stroke 2003;34:2221–7.
[6] Hua Y, Schallert T, Keep RF, Wu J, Hoff JT, Xi G. Behavioral tests after intracerebral hemorrhage in the rat. Stroke 2002;33:2478–84.
[7] Chen J, Li Y, Wang L, Zhang Z, Lu D, Lu M, et al. Therapeutic benefit of intravenous administration of bone marrow stromal cells after cerebral ischemia in rats. Stroke 2001;32:1005–11.
[8] James ML, Warner DS, Laskowitz DT. Preclinical models of intracerebral hemorrhage: a translational perspective. Neurocrit Care 2008;9:139–52.
[9] Hartman R, Lekic T, Rojas H, Tang J, Zhang JH. Assessing functional outcomes following intracerebral hemorrhage in rats. Brain Res 2009;1280:148–57.
[10] MacLellan CL, Silasi G, Poon CC, Edmundson CL, Buist R, Peeling J, et al. Intracerebral hemorrhage models in rat: comparing collagenase to blood infusion. J Cereb Blood Flow Metab 2008;28:516–25.
[11] Nakamura T, Keep RF, Hua Y, Schallert T, Hoff JT, Xi G. Deferoxamine-induced attenuation of brain edema and neurological deficits in a rat model of intracerebral hemorrhage. J Neurosurg 2004;100:672–8.
[12] MacLellan CL, Auriat AM, McGie SC, Yan RH, Huynh HD, De Butte MF, et al. Gauging recovery after hemorrhagic stroke in rats: implications for cytoprotection studies. J Cereb Blood Flow Metab 2006;26:1031–42.
[13] Farr TD, Whishaw IQ. Quantitative and qualitative impairments in skilled reaching in the mouse (*Mus musculus*) after a focal motor cortex stroke. Stroke 2002;33:1869–75.
[14] Fouad K, Schnell L, Bunge MB, Schwab ME, Liebscher T, Pearse DD. Combining Schwann cell bridges and olfactory-ensheathing glia grafts with chondroitinase promotes locomotor recovery after complete transection of the spinal cord. J Neurosci 2005;25:1169–78.
[15] Angeby-Moller K, Berge OG, Hamers FP. Using the CatWalk method to assess weight-bearing and pain behaviour in walking rats with ankle joint monoarthritis induced by carrageenan: effects of morphine and rofecoxib. J Neurosci Methods 2008;174:1–9.
[16] Vrinten DH, Hamers FF. 'CatWalk' automated quantitative gait analysis as a novel method to assess mechanical allodynia in the rat; a comparison with von Frey testing. Pain 2003;102:203–9.
[17] Bozkurt A, Deumens R, Scheffel J, O'Dey DM, Weis J, Joosten EA, et al. CatWalk gait analysis in assessment of functional recovery after sciatic nerve injury. J Neurosci Methods 2008;173:91–8.
[18] Chuang CS, Su HL, Cheng FC, Hsu SH, Chuang CF, Liu CS. Quantitative evaluation of motor function before and after engraftment of dopaminergic neurons in a rat model of Parkinson's disease. J Biomed Sci 2010;17:9.
[19] Encarnacion A, Horie N, Keren-Gill H, Bliss TM, Steinberg GK, Shamloo M. Long-term behavioral assessment of function in an experimental model for ischemic stroke. J Neurosci Methods 2011;196:247–57.
[20] Otero L, Zurita M, Bonilla C, Aguayo C, Vela A, Rico MA, et al. Late transplantation of allogeneic bone marrow stromal cells improves neurologic deficits subsequent to intracerebral hemorrhage. Cytotherapy 2011;13:562–71.
[21] Schallert T, Fleming SM, Leasure JL, Tillerson JL, Bland ST. CNS plasticity and assessment of forelimb sensorimotor outcome in unilateral rat models of stroke, cortical ablation, Parkinsonism and spinal cord injury. Neuropharmacology 2000;39:777–87.
[22] Ishida A, Tamakoshi K, Hamakawa M, Shimada H, Nakashima H, Masuda T, et al. Early onset of forced impaired forelimb use causes recovery of forelimb skilled motor function but no effect on gross sensory-motor function after capsular hemorrhage in rats. Behav Brain Res 2011;225:126–34.
[23] Hamers FP, Lankhorst AJ, van Laar TJ, Veldhuis WB, Gispen WH. Automated quantitative gait analysis during overground locomotion in the rat: its application to spinal cord contusion and transection injuries. J Neurotrauma 2001;18:187–201.
[24] Koopmans GC, Deumens R, Honig WM, Hamers FP, Steinbusch HW, Joosten EA. The assessment of locomotor function in spinal cord injured rats: the importance of objective analysis of coordination. J Neurotrauma 2005;22:214–25.
[25] Hendriks WT, Eggers R, Ruitenberg MJ, Blits B, Hamers FP, Verhaagen J, et al. Profound differences in spontaneous long-term functional recovery after defined spinal tract lesions in the rat. J Neurotrauma 2006;23:18–35.
[26] Koopmans GC, Deumens R, Brook G, Gerver J, Honig WM, Hamers FP, et al. Strain and locomotor speed affect over-ground locomotion in intact rats. Physiol Behav 2007;92:993–1001.
[27] Cendelin J, Voller J, Vozeh F. Ataxic gait analysis in a mouse model of the olivocerebellar degeneration. Behav Brain Res 2010;210:8–15.
[28] Tauber SC, Ribes S, Ebert S, Heinz T, Fingerle V, Bunkowski S, et al. Long-term intrathecal infusion of outer surface protein C from *Borrelia burgdorferi* causes axonal damage. J Neuropathol Exp Neurol 2011;70:748–57.
[29] Starkey ML, Barritt AW, Yip PK, Davies M, Hamers FP, McMahon SB, et al. Assessing behavioural function following a pyramidotomy lesion of the corticospinal tract in adult mice. Exp Neurol 2005;195:524–39.
[30] Gensel JC, Tovar CA, Hamers FP, Deibert RJ, Beattie MS, Bresnahan JC. Behavioral and histological characterization of unilateral cervical spinal cord contusion injury in rats. J Neurotrauma 2006;23:36–54.
[31] Gabriel AF, Marcus MA, Honig WM, Walenkamp GH, Joosten EA. The CatWalk method: a detailed analysis of behavioral changes after acute inflammatory pain in the rat. J Neurosci Methods 2007;163:9–16.
[32] Westin JE, Janssen ML, Sager TN, Temel Y. Automated gait analysis in bilateral Parkinsonian rats and the role of L-DOPA therapy. Behav Brain Res 2012;226:519–28.
[33] Dai H, Macarthur L, McAtee M, Hockenbury N, Das P, Bregman BS. Delayed rehabilitation with task-specific therapies improves forelimb function after a cervical spinal cord injury. Restor Neurol Neurosci 2011;29:91–103.
[34] Hamers FP, Koopmans GC, Joosten EA. CatWalk-assisted gait analysis in the assessment of spinal cord injury. J Neurotrauma 2006;23:537–48.
[35] Singh A, Murray M, Houle JD. A training paradigm to enhance motor recovery in contused rats: effects of staircase training. Neurorehabil Neural Repair 2011;25:24–34.
[36] Hoffmann MH, Hopf R, Niederreiter B, Redl H, Smolen JS, Steiner G. Gait changes precede overt arthritis and strongly correlate with symptoms and histopathological events in pristane-induced arthritis. Arthritis Res Ther 2010;12:R41.
[37] Ng SS, Hui-Chan CW. The timed up & go test: its reliability and association with lower-limb impairments and locomotor capacities in people with chronic stroke. Arch Phys Med Rehabil 2005;86:1641–7.
[38] Hsu AL, Tang PF, Jan MH. Analysis of impairments influencing gait velocity and asymmetry of hemiplegic patients after mild to moderate stroke. Arch Phys Med Rehabil 2003;84:1185–93.
[39] Aruin AS, Hanke TA, Sharma A. Base of support feedback in gait rehabilitation. Int J Rehabil Res 2003;26:309–12.
[40] Bensoussan L, Viton JM, Barotsis N, Delarque A. Evaluation of patients with gait abnormalities in physical and rehabilitation medicine settings. J Rehabil Med 2008;40:497–507.
[41] Graham HK, Baker R, Dobson F, Morris ME. Multilevel orthopaedic surgery in group IV spastic hemiplegia. J Bone Joint Surg Br 2005;87:548–55.
[42] Glajch KE, Fleming SM, Surmeier DJ, Osten P. Sensorimotor assessment of the unilateral 6-hydroxydopamine mouse model of Parkinson's disease. Behav Brain Res 2012;230:309–16.
[43] Spinazzola L, Cubelli R, Della Sala S. Impairments of trunk movements following left or right hemisphere lesions: dissociation between apraxic errors and postural instability. Brain 2003;126:2656–66.
[44] Del Bigio MR, Yan HJ, Buist R, Peeling J. Experimental intracerebral hemorrhage in rats. Magnetic resonance imaging and histopathological correlates. Stroke 1996;27:2312–9 [discussion 9–20].
[45] Guzman R, Meyer M, Lovblad KO, Ozdoba C, Schroth G, Seiler RW, et al. Striatal grafts in a rat model of Huntington's disease: time course comparison of MRI and histology. Exp Neurol 1999;156:180–90.